Journal of Organometallic Chemistry 734 (2013) 53–60

Contents lists available at SciVerse ScienceDirect

Journal of Organometallic Chemistry

journal homepage: www.elsevier.com/locate/jorganchem

Relative rates of reaction of Pt(en)Cl $(NH_2R)^+$ with guanosine monophosphate as a function of amino group substituent: Toward efficient labeling of DNA for TEM imaging

Rakesh Kumar [a], Edward Rosenberg [a,*], Miriam Inbar Feske [b], Antonio G. DiPasquale [c]

[a] Department of Chemistry, University of Montana, Missoula, MT 59812, USA
[b] Latham and Watkins, Menlo Park, CA 94025, USA
[c] Department of Chemistry, University of California, Berkeley, CA 94720, USA

ARTICLE INFO

Article history:
Received 28 September 2012
Received in revised form
30 October 2012
Accepted 1 November 2012

Keywords:
Platinum complexes
DNA
TEM
dGMP
Osmium clusters

ABSTRACT

In an attempt to understand the factors that govern the rates of reaction of the complexes [Pt(en)Cl$(NH_2R)]^+NO_3^-$ (en = ethylene diamine) with guanosine monophosphate (dGMP) a series of amine complexes, where R=$C_8H_9NO_2$ (benzo[*d*][1,3]dioxol-5-ylmethanamine) (**1**), $C_8H_{11}N$ (phenethylamine) (**2**), C_7H_9N (benzylamine) (**3**), C_6H_7N (aniline) (**4**), C_6H_6IN (*p*-iodo-aniline) (**5**) C_3H_9NO (2-methoxy-ethylamine) (**6**) and $C_6H_{13}N$ (cyclohexylamine) (**7**), were synthesized and their reactions with deoxy-guanosine monophosphate (dGMP) were followed by ^1H NMR. Compound **1** was initially chosen because it showed significant water solubility. Compound **1** reacted quantitatively but slowly with dGMP and a subsequent Transmission Electron Microscopy (TEM) study of the binding **1** to a GATC DNA repeat gave a TEM micrograph that showed selective labeling of DNA at guanine, using a technique that allowed the laying down of a straight single strand of DNA on a carbon platform. The TEM suggested a possible side reaction with adenine and so a study of the reaction of **1** with adenine was performed and showed slow and what appeared to be non-specific binding to deoxyadenosine monophosphate (dAMP). The reactions of compounds **2**–**7** with dGMP were then studied by ^1H NMR and it was found that **2** reacted much faster than **1** with dGMP while the remaining complexes reacted more slowly. No reaction of **2** with dAMP was observed in the same time frame. The ultimate goal of the project was to bind a third row transition metal cluster to guanine and given the effective binding of **1** to DNA the synthesis of the complex $[Os_3(CO)_{11}PPh_2(CH_2)_2NH_2(en)PtCl]NO_3$ (**9**) is also reported that contains Pt as a linker to label guanine. The synthesis was performed by reacting $Os_3(CO)_{10}(CH_3CN)_2$ with $Ph_2PCH_2CH_2NH_2$ which gave an η^2 chelate complex $Os_3(CO)_{10}PPh_2(CH_2)_2NH_2$ (**8**). Complex **8** was reacted with [Pt(en)Cl(DMF)]NO_3 in a CO atmosphere to give **9**. ^1H and ^{195}Pt NMR indicate formation of an adduct with dGMP but too slowly to be of use in labeling DNA. The solid-state structure of **8** is also reported.

1. Introduction

Beer and Moudrianakis (1962) first suggested that it may be possible to sequence DNA with the aid of the electron microscope [1]. Transmission Electron Microscopy (TEM) has the potential to bring the base pair reading length up to 10^5 base-pairs per minute if the bases could be specifically labeled with heavy atoms. Long reading length enables detection of long repeating patterns in the genetic code and facilitates high-speed sequencing. Hence, the cost of DNA sequencing can be reduced significantly with the use of TEM. DNA has only light element (C,H,N,O,P), that are inherently transparent to TEM. Heavy metal ($Z > 70$) staining is well known to increase image contrast in TEM, and heavy metal salts have long been used in TEM to render nucleic acids visible [1–4]. The relative number of electrons that are scattered to a detector is approximately proportional to $Z^{1.5}$. The inherent drawback in using metal salts' staining is the lack of specificity to a nucleotide base owing to non-specific interactions. Therefore, covalent adduct formation between a DNA base and a metal complex is necessary for determination of the position of a specific base in a DNA molecule, Thus, functionalized heavy metal complexes capable of base-specific labeling of DNA can provide a tool for DNA sequencing. Furthermore, the labels need to have high reactivity to attach themselves specifically to one of the four bases, GATC, along with very high

* Corresponding author.
E-mail address: edward.rosenberg@mso.umt.edu (E. Rosenberg).

0022-328X/$ – see front matter © 2012 Elsevier B.V. All rights reserved.
http://dx.doi.org/10.1016/j.jorganchem.2012.11.003

specificity. The key to getting sequence information from the heavy atom labeling is the ability to stretch a single strand of DNA onto a platform where multiple images of the strands can be added together to give the exact sites of heavy atom labeling. Recently, such a technique has been developed, by Halcyon Molecular and provided the opportunity to develop heavy atom labels for DNA [5]. We have been studying the interaction of benzoheterocycle complexes of triosmium carbonyl clusters for the last ten years [6–8]. These studies revealed some of the structural requirements for selective binding of modified triosmium clusters with guanosine monophosphate (dGMP). Selectivity for guanine over the other bases was also observed [7,8]. However, subsequent attempts to obtain a straight and stretched single stranded DNA containing a covalently bound triosmium cluster failed. In order to demonstrate proof of concept for the technique of visualizing a guanine bound metal complex on DNA with TEM we studied the reaction of the complexes $[Pt(en)Cl(NH_2R)]^+NO_3^-$ with dGMP and DNA. It was previously been shown that complexes of this type were selective for binding to guanine when R was a luminescent molecule [9]. We report here the successful visualization of the Pt atoms in the complex $[Pt(en)Cl(NH_2R)]^+NO_3^-$ (R═$C_8H_9NO_2$ (benzo[*d*][1,3]dioxol-5-ylmethanamine, also known as piperonylamine) (**1**)) bound to DNA by TEM as well as a qualitative kinetic study of a series of related complexes reacting with dGMP and the synthesis and dGMP binding of a Pt-triosmium conjugate.

2. Results

2.1. Synthesis of *1* and its reaction with dGMP

Complex **1** was synthesized by the reaction of benzo[*d*][1,3]dioxol-5-ylmethanamine with $[(en)PtCl_2]$ via halide abstraction in dimethylformamide (Equation (1)).

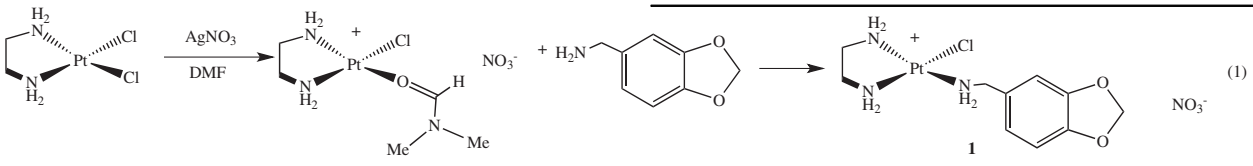

The complex was characterized by ^1H, ^{195}Pt NMR and mass spectrometry. The ^{195}Pt NMR of the DMF intermediate complex showed two overlapping resonances in DMF/THF-d^8 which we attribute to a mixture of the DMF and THF-d^8 complexes (Fig. 1a). To this solution was added 0.8 equivalents of piperonylamine, the solution evaporated to dryness and dissolved in D_2O. The ^{195}Pt NMR showed a single peak at −2625 ppm relative to chloroplatinic acid (Fig. 1b) [10]. To this solution of **1** was added an equimolar (based on the piperonylamine) amount of dGMP and a shift to −2511 ppm was observed (Fig. 1c). This gives evidence for the formation of a single adduct of **1** with dGMP.

2.2. The reaction of *1* with dGMP followed by ^1H NMR

Equimolar solutions of **1** and dGMP were combined in D_2O and the reaction followed by ^1H NMR over the course of 24 h using solvent suppression for the HDO peak (Fig. 2). Resonances assignable to residual DMF were observed at 8.3 ppm (CH) and 2.3 and 2.4 ppm (2 Me). Thirty minutes after addition of dGMP a new resonance appeared at 8.5 ppm downfield of the H(8) of dGMP at 7.9 ppm which we assign to the formation of the adduct **1-dGMP** (Equation (2)).

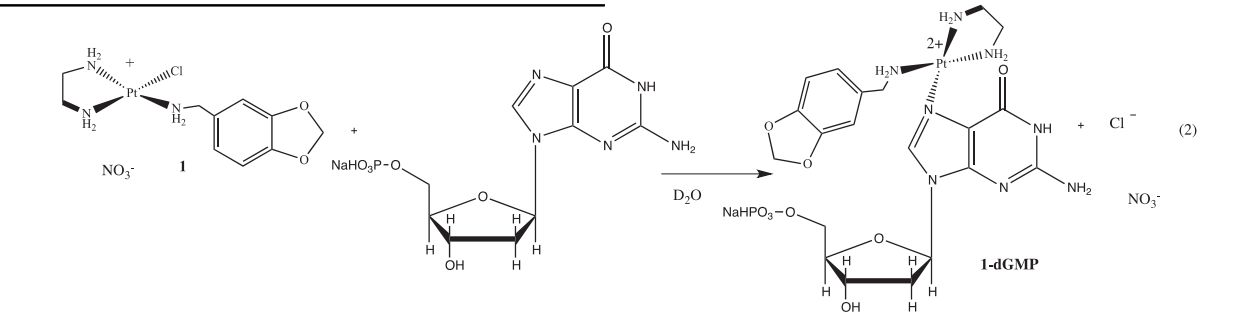

With increasing time the resonance at 7.9 ppm continues to decrease while the resonance at 8.5 ppm. After 19 h the resonance at 7.9 ppm has completely disappeared and only the peak assignable to **1-dGMP** is observed accompanied by the DMF resonance at 8.3 ppm in the downfield region of the spectrum. Other changes in the resonances above 7.0 ppm also observed.

2.3. Transmission electron microscopy of *1* incubated with ss-DNA GATC repeat

Based on these results **1** was incubated with a 25 mmol solution of a single-stranded GATC repeat (60 bases in length) at 40 °C for 6 h in aqueous phosphate buffer using a six-fold molar excess of label (compound **1**) relative to the number of guanines. After dialysis to remove excess label a micro drop of the solution was subjected to the stretching and straightening technique developed by Halcyon Molecular [5]. Multiple strands were deposited on glass slide, sprayed with carbon and imaged on the 300 kV VG Microscope at Oak Ridge National Lab [11]. Fig. 3 shows a TEM image of a segment of the labeled GATC repeat. There are 15 G bases in the segment using the calculated value 0.77 nm/base and 11 of them are labeled (green dots). There are several labels that are out of sequence (red dots) and these could be labeled adenines.

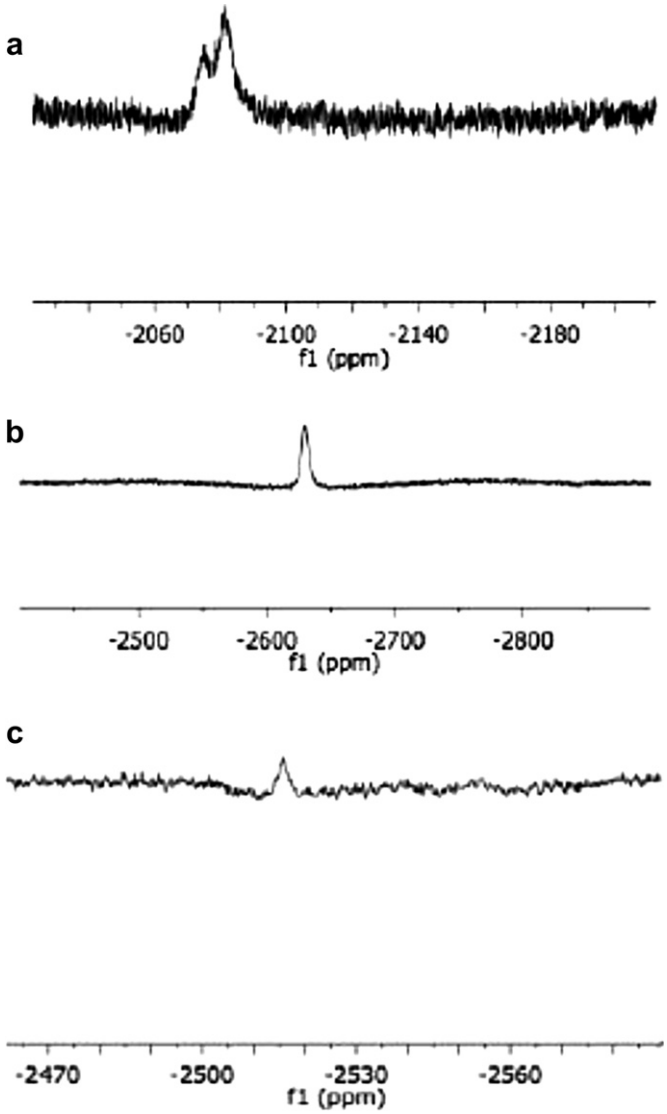

Fig. 1. a) ^{195}Pt NMR of [Pt(en)Cl(DMF)]NO_3 in THF-d^4/DMF. b) ^{195}Pt NMR of [Pt(en)Cl(piperonyl)]NO_3 in D_2O. c) ^{195}Pt NMR of [Pt(en)Cl(piperonyl)]NO_3 + dGMP in D_2O.

2.4. ^{1}H NMR studies of **1** with dAMP

In order to test this hypothesis the reaction of deoxyadenosine monophosphate (dAMP) with **1** was studied. The ^{1}H NMR of equimolar amounts of dAMP and **1** in D_2O was followed over a 24 h period using water suppression. Although evidence of reaction is observed in the form of new resonances appearing in the downfield (8 ppm) and upfield (2–7 ppm) regions of the spectrum the H(8) of the adenine is still present after 24 h (Fig. 4). Thus the reaction **1** with dAMP is much slower than with dGMP and appears to be less specific, given the greater number new resonances that appeared over the 24 h period. Nonetheless, this experiment does lend credence to the idea that the outlier labels (red dots) are **1-dAMP** although it is not clear if this product has the same structure as **1-dGMP** (Equation (2)). Monofunctional Pt complexes give simpler Pt-G monoadducts.

N7 of both adenine and guanine can be platinated, however N7 of guanine shows a greater kinetic preference. This tendency results from the stronger basicity of that nitrogen and from possible simultaneous hydrogen-bond interactions between NH_3^+ protons and the O(6) of guanine. In contrast, in the case of adenine, only repulsive interactions can be produced between the NH_2 in position 6 of adenine and a platinum-bonded amine ligand [9].

2.5. Kinetic studies of amine variants, compounds **2**–**7**, with dGMP

The TEM experiment constitutes a proof of concept in that it illustrates that it is possible to visualize a single platinum atom with base selectivity, bound to stretched single-stranded DNA. However, for this labeling scheme to be effective the reaction of **1** with dGMP must be much faster. To this end, a study of the rates of reaction of a series of complexes related to **1**, Pt(en)Cl(NH_2R)]$^+NO_3$ where R= $C_8H_{11}N$ (phenethylamine) (**2**), C_7H_9N (benzylamine) (**3**), C_6H_7N (aniline) (**4**), C_6H_6IN (*p*-iodo-aniline) (**5**) C_3H_9NO (2-methoxy-ethylamine) (**6**) and $C_6H_{13}N$ (cyclohexylamine) (**7**) were synthesized and their rates of reaction with dGMP were followed by ^{1}H NMR (Chart 1). The amines were chosen for their differences in steric bulk and basicity of the donor atom. The aromatic amines in this series were chosen based on the prior work of Heetebrij et al. who found that aromatic amines showed a higher affinity for guanine relative to the other bases and attributed this to π-stacking effects [9]. The aliphatic amines used were chosen for comparison to see how important the stacking effect was for the rate of reaction as well as the selectivity. In the case of **5** a second heavy atom was included to increase electron scattering to improve visualization of the label. The experiments were conducted with equimolar amounts of the amine complexes and dGMP in D_2O with water suppression. The reaction of **2** with dGMP is shown in Fig. 5 and it can be seen that it reacts much more quickly **1**, with the reaction being almost complete after just 2 h. Fig. 6 compares the rate of conversion of **1** with **2** and **4**. Complex **3** showed the same rate of conversion as **1**, both being benzyl amines. Fig. 7 compares the rate of conversion of **4** with **5** and shows that inclusion of the iodine atom does not have huge influence on the initial rate but does decrease the overall % conversion after 24 h. Complexes **6** and **7** reacted only sluggishly with dGMP and showed <50% after 24 h. It is clear from these results that the longer tether in the phenethylamine complex results in the fastest rate of conversion and represents the best candidate for single metal atom labeling of guanine in single-stranded DNA.

2.6. Synthesis and structure [$Os_3(CO)_{10}PPh_2(CH_2)_2NH_2$] (**8**)

The studies with complexes **1**–**5** showed that a two-carbon tether gave the best rate of conversion. However, visualizing a single heavy metal atom label would require the very powerful TEM located at ORNL [11]. In the hope of combining the effectiveness of the two-carbon tether with a metal cluster label, which would allow in-house imaging with more conventional TEM instruments, we synthesized the compound [$Os_3(CO)_{11}PPh_2(CH_2)_2NH_2$(en)PtCl]$NO_3$ (**9**) using the bidentate ligand 2-diphenylphosphino-ethylamine (Scheme 1). $Os_3(CO)_{11}(CH_3CN)$ [12] was reacted with 2-diphenylphosphino-ethylamine at ambient temperature in methylene chloride. The spectroscopic data indicated that the reaction had resulted in the displacement of a carbonyl ligand to give [$Os_3(CO)_{10}PPh_2(CH_2)_2NH_2$] (**8**) (Scheme 1). However, we could not determine if the ligand was coordinated in a bridging or chelating mode and so a solid-state structure was undertaken. The solid-state structure of **8** is shown in Fig. 7 with selected bond lengths and angles in the figure caption. The crystal and collection data are given in Table 1. The 2-diphenylphosphino-ethylamine ligand is chelated to one Os atom. There is considerable precedent in the literature for the chelate structure being preferred for bidentate ligands with an ethylene bridge in the chemistry of triosmium clusters. However, the equilibrium between the chelate and two metal atom bridging structure is highly dependent on the nature of the of the two donor

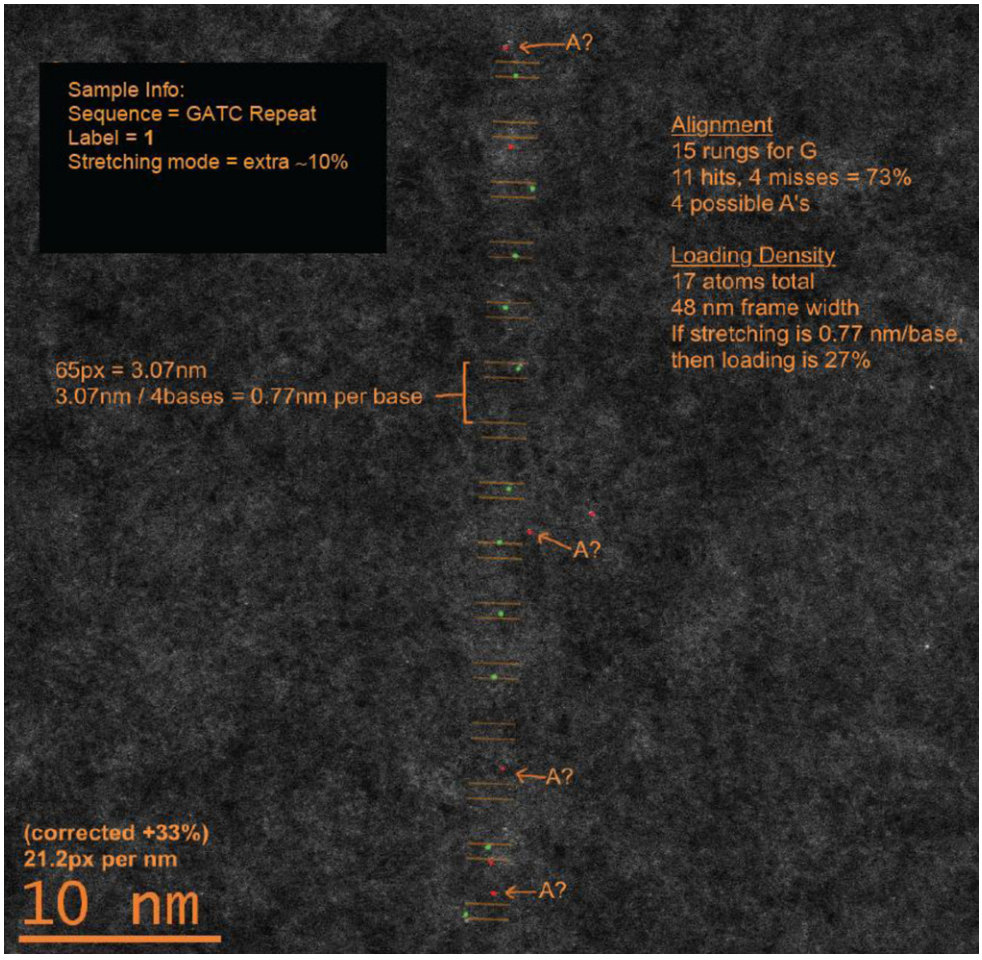

Fig. 2. ^{1}H NMR of **1** + equimolar dGMP versus time.

atoms, i.e. (PP), (PS), (PN) or (PO) [13–17]. The structure of **8** consists of an Os triangle with the chelating diphenylphosphino-2-ethylamine ligand on Os(3). The Os(2)–Os(3) bond length is slightly shorter than (2.86(2) Å) than the other two Os–Os bonds (2.91(2) Å.) The Os(3)–P(1) and Os(3)–(N1) bond lengths (2.32(2) and 2.25(2) Å) respectively are fairly typical of these bonds in triosmium clusters [14–18].

2.7. Conversion of (**8**) to $[Os_3(CO)_{11}PPh_2(CH_2)_2NH_2(en)PtCl]NO_3$ (**9**) and attempted reaction with dGMP

The opening of the chelate ring at the Os(3)–N(1) bond could be accomplished by treating **8** with CO gas at 50 °C in THF-d^{8}. The reaction is followed by ^{31}P NMR and after 1 h the ^{31}P NMR resonance at 33.70 ppm assigned to **8** is replaced by a new resonance at 35.55 ppm. To the THF solution was added an equimolar amount of

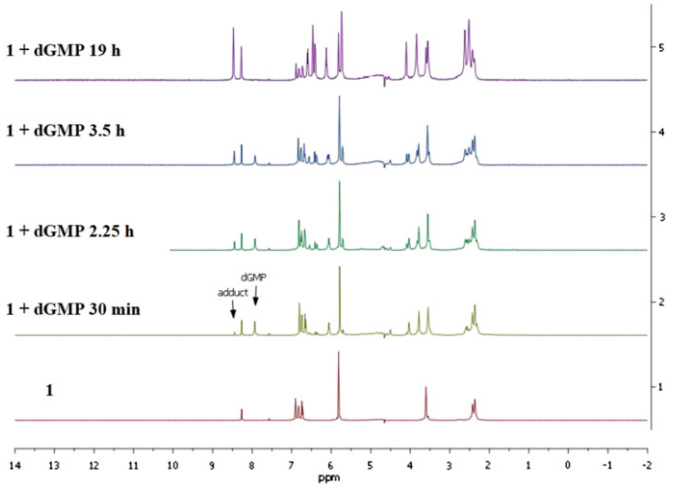

Fig. 3. TEM image of **1** incubated with a GATC repeat using a 300 kV VG microscope at Oak Ridge National lab.

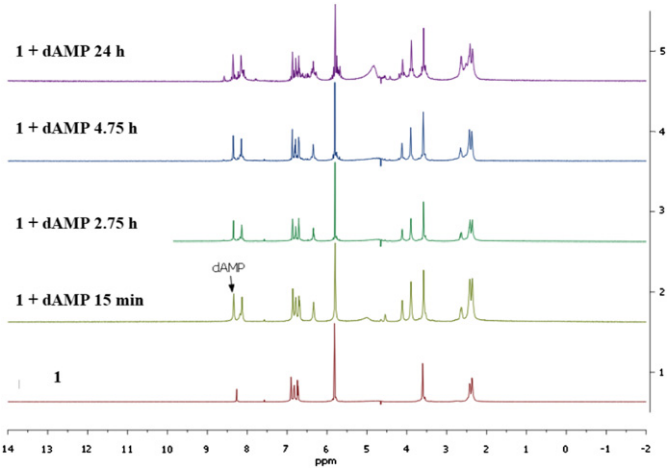

Fig. 4. ^{1}H NMR studies of **1** + equimolar dAMP versus time.

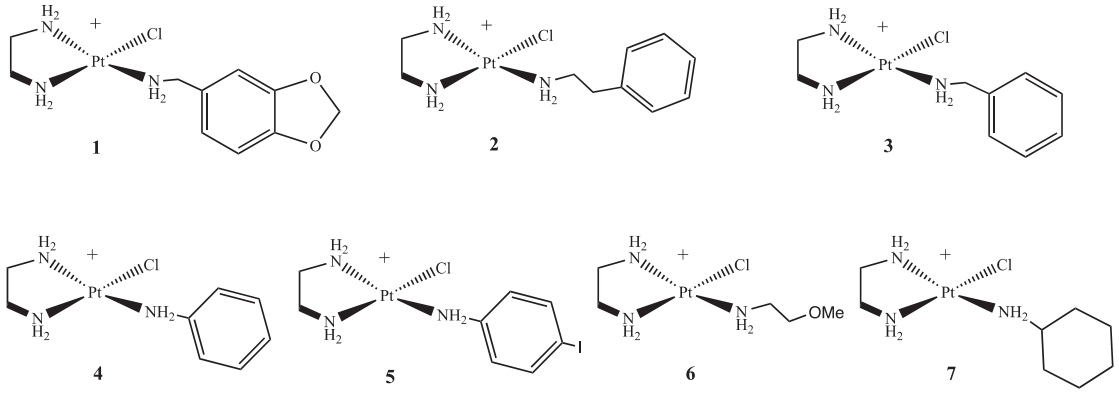

Chart 1.

[Pt(en)Cl(DMF)]NO_3. The Pt-cluster adduct was isolated by preparative reverse phase TLC and characterized by IR and NMR spectroscopies as $[Os_3(CO)_{11}PPh_2(CH_2)_2NH_2(en)PtCl]NO_3$ (**9**).

A solution of **9** was then combined with an equimolar amount of dGMP in 90:10 D_2O:CD_3OD. After 4 h there was some evidence of formation of an adduct as noted by the appearance of a new resonance at 8.6 ppm downfield of the H(8) resonance of guanine as noted for the other dGMP adducts reported here. However with increasing time a precipitation was noted and the overall intensity of the NMR resonances increased. Thus it appears that if **dGMP-9** its solubility in this solvent mixture was too limited to make further studies possible.

3. Discussion

The TEM results reported here for the labeling of GATC DNA with **1** using the stretching technique and the distance grid developed by Halcyon Molecular represents a proof of concept for visualizing a single platinum atom selectively bound to guanine [5]. The selectivity for guanine is based on the clear results of our studies in solution on the binding of **1** with dGMP. This selectivity is also based on our previous studies with dGMP and triosmium cluster labels [8]. Outlier spots were observed in the TEM and were attributed side reactions with adenine that could be due to either covalent bonding as with guanine or to non-specific electrostatic interactions. Following the reaction of dAMP with **1** resulted in much more complex changes in the ^{1}H NMR of the dAMP relative to dGMP suggesting that there are several ways that the dAMP is interacting with the label (Figs. 3 and 4).

Although **1** was reasonably selective for guanine its reaction with dGMP was rather slow. Following the rates of the reactions of complexes **2**–**7** revealed some of the factors that control the rate of reaction of these Pt complexes with DNA. Complex **2**, the phenethylamine analogue showed fastest reactivity as observed by NMR spectroscopy. It was consumed in 2 h compared to **1**, which took 12 h at RT. Complex **3** reacted at the same rate as **1** being a benzylamine, illustrating that the dioxo ring has little influence on the rate of reaction with dGMP, but is preferred for its better water solubility. Complex **4** reacted more slowly than **1** or **2** and taken together the results shown in Fig. 5 suggest that tether length to the aromatic ring is the dominant factor in affecting the rate of reaction with dGMP. The differences in basicity may also play a role but based on the results for the remaining complexes this is apparently of secondary importance. Complex **5** reacts more slowly than **4** and this may be due to the electron withdrawing effect of the iodo group (Fig. 6). This is unfortunate in that the iodo group would offer enhanced imaging possibilities. Complexes **6** and **7** reacted very slowly and reaction with dGMP was <50% converted after 24 h. We tentatively assign this to steric considerations where the greater motional degrees of freedom of **6** and the relative bulkiness of the cyclohexyl group in **7** compared to phenyl interferes with the displacement of chloride by the dGMP.

The synthesis of complexes **8** and **9** opens the way for the labeling of DNA bases with clusters attached to a platinum complex. However, water solubility of the **9-dGMP** conjugate or **9** itself presents a significant obstacle. Previous studies have shown

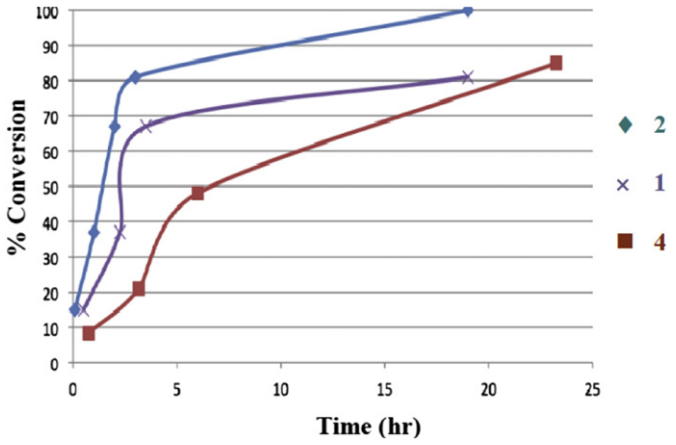

Fig. 5. Kinetic plots of the reaction complexes **1**, **2** and **4** with dGMP run at ambient temperatures in D_2O and based on integration of the adduct peak to the H(8) peak of dGMP relative to the HDO peak.

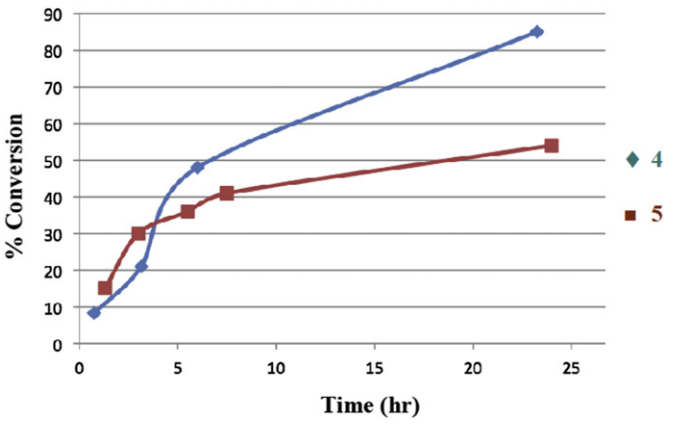

Fig. 6. Kinetic plots of the reaction complexes **4** and **5** with dGMP run at ambient temperatures in D_2O and based on integration of the adduct peak to the H(8) peak of dGMP relative to the HDO peak.

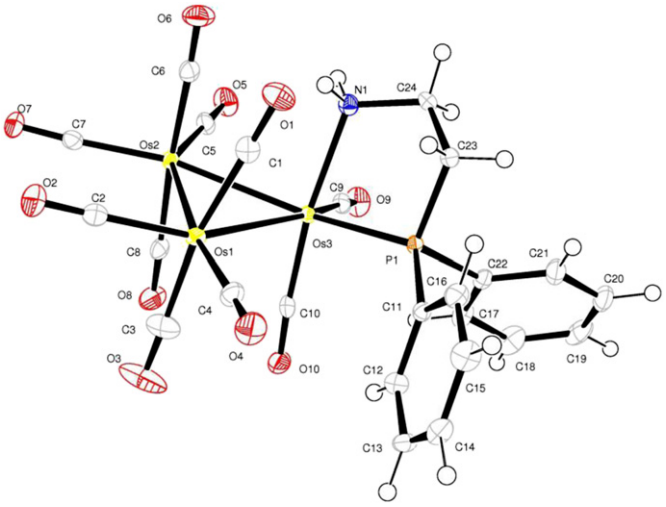

Fig. 7. Solid-state structure of $[Os_3(CO)_{10}PPh_2(CH_2)_2NH_2]$ (**8**). Selected bond distances: N(1)–Os(3), 2.249(3); N(1)–H(1A), 0.9200; N(1)–H(1B), 0.9200; P(1)–Os(3), 2.3206(9); Os(1)–Os(2), 2.9028(2); Os(1)–Os(3), 2.9151(2); Os(2)–Os(3), 2.8626(2) Å. Average CO bond distance: 1.147(5) Å. Average Os–C–O bond angle: 176.1(3) deg.

however that the introduction of water-soluble phosphines onto the cluster label causes distortion of the stretched single-stranded DNA making accurate calculations of the ladder grid impossible [19].

4. Conclusions

The relative rates reported here for the reactions of **1**–**7** with dGMP could prove useful for future applications of the reactions of Pt complexes with DNA. The visualization of **1** attached to a stretched single stranded DNA is proof of concept for the application of high-powered TEM for visualization of single metal atoms attached to bio-macromolecules. However, taken together with the other unpublished work done in collaboration with Halcyon Molecular it does not appear that fast throughput labeling using heavy atom labels and the DNA stretching technique will be a viable pathway for fast throughput genetic sequencing [20]. Other techniques appear to be much further down this path [21].

5. Experimental

5.1. Materials

All amines, TMAO (trimethylamine N-oxide), $Pt(en)Cl_2$, dAMP and dGMP were purchased from Sigma–Aldrich Chemicals and used as received. Osmium carbonyl and diphenylphophino-2-ethylamine were purchased from Strem Chemicals and used as received. Deuterated solvents were purchased from Cambridge Isotopes Inc and used as received. Acetonitrile and methylene chloride were distilled from calcium hydride directly before use. Other solvents were reagent grade and were purchased from J. T. Baker and used as received. Syntheses of the Os-cluster compounds carried out under a nitrogen atmosphere, but purification processes were carried out in air using preparative thin layer chromatography (20 × 20 cm plates coated with 500 μm silica from Dynamic Absorbents or Uniplate reverse phase, hydrocarbon impregnated silica gel 1000 μm).

5.2. Methods

^1H, ^{195}Pt and ^{31}P NMR spectra were obtained on a Varian NMR system 500 MHz spectrometer at 500, 109.1 and 202.6 MHz respectively. Infrared spectra were obtained on a Thermo-Nicolet 633 FT-IR spectrometer. Prior to the NMR experiments all Pt complexes (except **9**) were purified on a Biotage (Isolera prime Flash purification system)

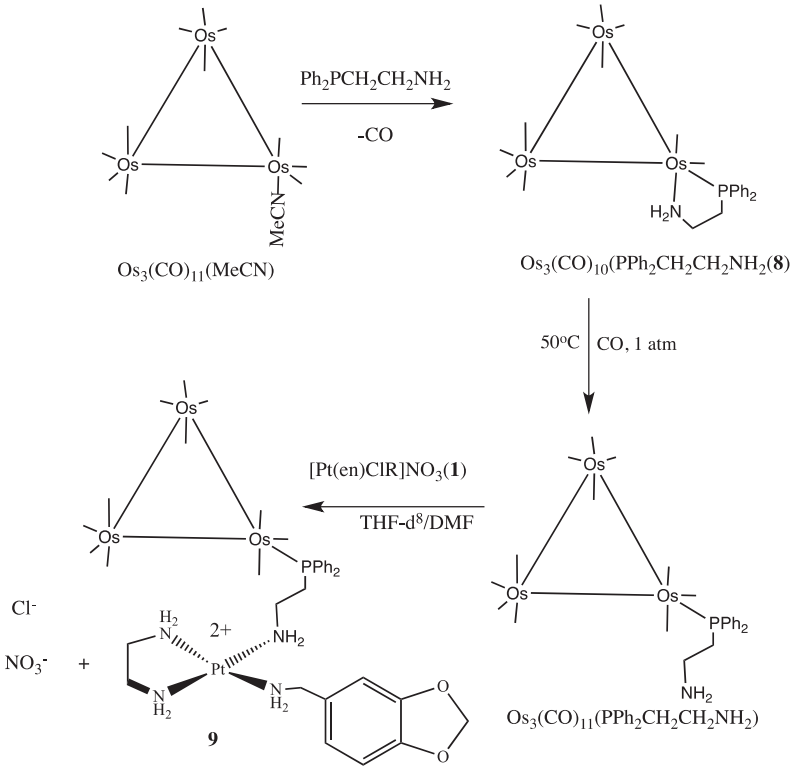

Scheme 1.

Table 1
Crystal data and structure refinement for compound **8**.

Empirical formula	$C_{24}H_{16}NO_{10}Os_3P$	
Formula weight	1079.95	
Temperature	100(2) K	
Wavelength	0.71073 Å	
Crystal system	Monoclinic	
Space group	P2(1)/*n*	
Unit cell dimensions	$a = 8.9448(3)$ Å	$\alpha = 90°$
	$b = 14.7147(4)$ Å	$\beta = 101.5820(10)°$
	$c = 20.9890(7)$ Å	$\gamma = 90°$
Volume	2706.32(15) Å^3	
Z	4	
Density (calculated)	2.651 Mg/m^3	
Absorption coefficient	14.165 mm^{-1}	
F(000)	1960	
Crystal size	0.07 × 0.05 × 0.04 mm^3	
Crystal color/habit	Yellow plate	
Theta range for data collection	1.70–25.39°	
Index ranges	$-10 \le h \le 10$, $-17 \le k \le 17$, $-24 \le l \le 25$	
Reflections collected	50804	
Independent reflections	4970 [R(int) = 0.0318]	
Completeness to theta = 25.00°	100.0%	
Absorption correction	Semi-empirical from equivalents	
Max. and min. transmission	0.6011 and 0.4372	
Refinement method	Full-matrix least-squares on F^2	
Data/restraints/parameters	4970/0/352	
Goodness-of-fit on F^2	1.128	
Final R indices [I > 2sigma(I)]	R1 = 0.0150, wR2 = 0.0299	
R indices (all data)	R1 = 0.0187, wR2 = 0.0315	
Largest diff. peak and hole	0.844 and −0.798 e Å^{-3}	

using Chromobond Flash FM 15/2 C_{18}, 9 cm and Chromobond Flash FM 25/5 C-18, 10 cm columns. Mass spectra for the amine complexes were obtained on a Shimadzu LCMS 2020. The mass spectrum for compound **8** was obtained on a Waters e2695 separation module combined with a Micromass technologies LCT Premier XE.

5.3. Syntheses

5.3.1. [Pt(en)Cl(DMF)]NO_3

[Pt(en)Cl_2] (50 mg, 0.153 mmol) was suspended in DMF (5 mL) and $AgNO_3$ (24.8 mg, 0.146 mmol, 0.95 equiv.) in DMF (1 mL) was added. The solution was stirred for 16 h at room temperature in the dark and filtered through membrane filters (0.2 μm) to remove AgCl.

5.3.2. [Pt(II)(piperonylamine)(en)Cl]$^+NO_3^-$ (**1**)

Piperonylamine (18.5 mg, 0.122 mmol, 0.8 equiv relative to [Pt(en)Cl_2]) was dissolved in xylene (12 mL) and added to the [Pt(en)Cl(DMF)]$^+NO_3^-$ solution. The mixture was stirred overnight at 40 °C. Solvents were removed *en vacuo* and the remaining product was redissolved in a minimum amount of Milli-Q water and stored overnight at 4 °C. Insoluble yellow particles of residual [Pt(en)Cl(dmf)]$^+NO_3^-$ were removed by filtration through membrane filters (0.2 μm). The clear filtrate was lyophilized to give the final product (**1**) in approximately 45% yield. ^{1}H NMR (D_2O, 500 MHz, 298 K): δ 2.2 (s, $3NH_2$, en), 2.6 (s, en), 3.6 (s, CH_2), 5.8 (s, CH_2 ppr), 6.7 (s, CH, Ar), 6.8 (s, CH, Ar), 6.9 (s, CH, Ar). ^{195}Pt NMR (D_2O, 500 MHz, 298 K) δ −2624.8. MS (ES): *m*/*z* 443.

5.3.3. 1-dGMP

In an NMR tube **1** (4.5 mg, 0.089 mmol, 1 equiv.) and dGMP (3.0 mg, 0.089 mmol, 1 equiv.) were mixed in 0.5 mL D_2O. The mixture was kept at 40 °C for overnight. A new resonance at −2511 ppm appeared in ^{195}Pt NMR and the −2625 ppm peak disappeared completely.

In a separate reaction the reaction was followed by ^{1}H NMR a new peak appeared at δ 8.2 and 7.9 H(8) peak disappeared completely.

5.3.4. [Pt(II)phenethylamine(en)Cl](NO_3) (**2**)

Phenethylamine (14.7 mg, 0.122 mmol, 0.8 equiv.) was dissolved in xylene (12 mL) and added to the [Pt(en)Cl(DMF)]NO_3 (0.122 mmol) solution. ^{1}H NMR (D_2O, 500 MHz, 298 K): δ 2.2 (s, $3NH_2$), 2.4 (s, en), 2.8 (s, CH_2), 2.9 (s, CH_2), 7.2 (m, CH_{phy}), 7.4 (m, CH_{phy}). MS (ES): *m*/*z* 412.

5.3.5. [Pt(II)benzylamine(en)Cl](NO_3) (**3**)

Benzylamine (13.07 mg, 0.122 mmol, 0.8 equiv.) was dissolved in xylene (12 mL) and added to the [Pt(en)Cl(DMF)]NO_3 (0.122 mmol) solution. ^{1}H NMR (D_2O, 500 MHz, 298 K): δ 2.0 (s, $3NH_2$), 2.8 (t, en), 3.8 (s, CH_2), 7.3 (m, CH, Ar). MS (ES): *m*/*z* 399.

5.3.6. [Pt(II)aniline(en)Cl](NO_3) (**4**)

Aniline (11.36 mg, 0.122 mmol, 0.8 equiv.) was dissolved in xylene (12 mL) and added to the [Pt(en)Cl(DMF)]NO_3 (0.122 mmol) solution. ^{1}H NMR (D_2O, 500 MHz, 298 K): δ 2.0 (s, $3NH_2$), 2.8 (t, en), 6.6 (m, CH, Ar), 6.8 (m, CH, Ar), 7.2 (m, CH, Ar). MS (ES): *m*/*z* 385.

5.3.7. [Pt(II)(4-iodoaniline)(en)Cl](NO_3) (**5**)

4-iodoaniline (27.72 mg, 0.122 mmol, 0.8 equiv.) was dissolved in xylene (12 mL) and added to the [Pt(en)Cl(DMF)]NO_3 (0.122 mmol) solution. ^{1}H NMR (D_2O, 500 MHz, 298 K): δ 2.0 (s, $3NH_2$), 2.8 (t, en), 6.4 (m, CH, Ar), 7.4 (m, CH, Ar). MS (ES): *m*/*z* 511.

5.3.8. [Pt(II)(2-methoxyethanamine)(en)Cl](NO_3) (**6**)

2-methoxyethanamine (9.16 mg, 0.122 mmol, 0.8 equiv.) was dissolved in xylene (12 mL) and added to the [Pt(en)Cl(DMF)]NO_3 (0.122 mmol) solution. ^{1}H NMR (D_2O, 500 MHz, 298 K): δ 2.0 (s, $3NH_2$), 2.7 (t, CH_2), 2.8 (s, en), 3.3 (s, CH_3), 3.8 (t, CH_2). MS (ES): *m*/*z* 377.

5.3.9. Pt(II)(cyclohexylamine)(en)Cl(NO_3) (**7**)

Cyclohexylamine (12.34 mg, 0.122 mmol, 0.8 equiv.) was dissolved in xylene (12 mL) and added to the [Pt(en)Cl(DMF)]NO_3 (0.122 mmol) solution. ^{1}H NMR (D_2O, 500 MHz, 298 K): δ 1.1 (m, CH_2), 1.5 (m, CH_2), 1.7 (m, CH_2), 2.0 (s, $3NH_2$), 2.7 (m, CH), 2.8 (s, en), 3.3 (s, CH_3), 3.8 (t, CH_2). MS (ES): *m*/*z* 391.

5.3.10. [$Os_3(CO)_{10}PPh_2(CH_2)_2NH_2$ (**8**)

[$Os_3(CO)_{11}(NCCH_3)$] [12] (370 mg, 0.402 mmol) was dissolved in 10 mL CH_2Cl_2 and $PPh_2(CH_2)_2NH_2$ (0.092 mg, 0.402 mmol) was added. The solution was stirred at room temperature for overnight. Analytical thin layer chromatography (30% CH_2Cl_2 and 70% hexane as eluent) was used to confirm complete conversion. The solution was rotary evaporated under vacuum to dryness. Two bands were observed on preparative TLC. Faster moving band gave a cyclized amino–phosphine complex **8**. Yield for **8**: 45%. IR ν(CO) in KBr:

2079 m, 2028 s, 2004 m, 1974 w cm^{-1}. ^1H NMR (500 MHz in CH_2Cl_2 at 25 °C) 7.53 (m, 3H, H(3,4,5)), 7.42 (m, 2H, H(2,6)), 2.43 (s (NH_2)), 1.56 (m, 2H, $CH_2\beta$-NH_2), 1.09 (m, 2H, $CH_2\alpha$-NH_2). ^{13}C NMR (CH_2Cl_2): 187.35 (s, 4CO), 187.45 (s, 4CO), 183.95 (s, 2CO). ^{31}P NMR (CH_2Cl_2): 33.70 (s, 1P, $PPh_2(CH_2)_2NH_2$). Mass spectrum: calcd 1090 amu; observed 1089 amu and 1112 (parent ion plus Na^+).

5.3.11. Chelate ring opening of **8** with CO complexation with [Pt(en)Cl(DMF)]NO_3

40 mg (0.036 mmol) of compound **8** dissolved in THF-d^8 (10 mL) and CO gas was bubbled through the solution at 50 °C for 1 h. The reaction was monitored by ^{31}P NMR spectroscopy the resonance at 33.70 ppm assignable to **8** shifted to 35.55 ppm which we assign to the ring-opened compound $[Os_3(CO)_{11}PPh_2(CH_2)_2NH_2]$. A solution of [Pt(en)Cl(DMF)]NO_3 (0.03 mmol) in 1.5 mL DMF was then added to the reaction flask and was stirred at room temperature for overnight. The Pt-cluster adduct was then precipitated with diethyl ether to remove DMF and purified by reverse phase preparative TLC (50% MeOH, 50% CH_2Cl_2). One faint band was observed and isolated by extraction with methanol and rotary evaporation. 35 mg (0.023 mmol) of a greenish-brown solid was obtained whose spectroscopic data is consistent with $[Os_3(CO)_{11}PPh_2(CH_2)_2NH_2(en)PtCl]NO_3$ (**9**). ν(CO) in KBr: 1966 m, 2003 s, 2047 m, 2081 w cm^{-1}. ^1H NMR (500 MHz in CD_3OD at 25 °C) 7.8–8.2 (broad m, 12H, Phen), 5.9 (s, 2H, NH_2), 3.6 (s, 2H, CH_2–P), 3.1(t, 4H, en), 1.6 (s, 2H, CH_2–N). ^{31}P NMR (CD_3OD) 35.55.

5.3.12. Reaction between dGMP and $[Os_3(CO)_{11}PPh_2(CH_2)_2NH_2(en)PtCl]NO_3$ (**9**)

Equimolar molar amounts of dGMP (0.023 mmol) and $[Os_3(CO)_{11}PPh_2(CH_2)_2NH_2(en)PtCl]NO_3$ (0.023 mmol) were added in CD_3OD and D_2O (90:10). Reaction was followed by ^1H NMR. Some conversion to **dGMP-9** was observed after 4 h as noted by the decrease in H(8) resonance of dGMP and the appearance of a new resonance at 8.6 ppm but due to precipitation of either the **dGMP-9** or **9**, conversion rate could not be followed precisely.

5.4. Solid-state structure determination of 8

A yellow plate 0.07 × 0.05 × 0.04 mm in size was mounted on a Cryoloop with Paratone oil. Data were collected in a nitrogen gas stream at 100(2) K using phi and omega scans. Crystal-to-detector distance was 60 mm and exposure time was 20 s per frame using a scan width of 1.0°. Data collection was 100.0% complete to 25.00° in θ. A total of 50804 reflections were collected covering the indices, $-10 \le h \le 10$, $-17 \le k \le 17$, $-24 \le l \le 25$. 4970 reflections were found to be symmetry independent, with an R_{int} of 0.0318. Indexing and unit cell refinement indicated a primitive, monoclinic lattice. The space group was found to be P2(1)/*n* (No. 14). The data were integrated using the Bruker SAINT software program and scaled using the SADABS software program. Solution by direct methods (SIR-97) produced a complete heavy-atom phasing model consistent with the proposed structure. All non-hydrogen atoms were refined anisotropically by full-matrix least-squares (SHELXL-97). All hydrogen atoms were placed using a riding model. Their positions were constrained relative to their parent atom using the appropriate HFIX command in SHELXL-97.

Acknowledgements

We gratefully acknowledge Halcyon Molecular and the University of Montana for support of this research and Christopher Own for help with the TEM imaging.

Appendix A. Supplementary materials

Crystallographic data for **8** have been deposited with the Cambridge Crystallographic Data Center CCDC No. 903534. Copies of the information may be obtained free of charge from the Director, CCDC, 12 Union Road, Cambridge, CB2 IEZ UK (fax: 44-1223-336-033); email: deposit@ccdc.ac.uk or http://wwwccdc.cam.ac.uk.

References

[1] M. Beer, E.N. Moudrianakis, Proc. Natl. Acad. Sci. U S A 48 (1962) 409.
[2] H.P. Erickson, M. Beer, Biochemistry 6 (1967) 2694. N. Y.
[3] J.P. Langmore, N.R. Cozzarelli, A.V. Crewe, Proc. Electron Microsc. Soc. Am. 30 (1972) 184.
[4] J.J. Frizell, J. Theor. Biol. 59 (1976) 241.
[5] W. Andregg, M. Andregg, PCT Int. Appl. (2009). WO 2009046445 A1 20090409.
[6] E. Rosenberg, F. Spada, K. Sugden, B. Martin, L. Milone, R. Gobetto, A. Viale, J. Fiedler, J. Organomet. Chem. 668 (2003) 51.
[7] E. Rosenberg, F. Spada, K. Sugden, B. Martin, R. Gobetto, L. Milone, A. Viale, J. Organomet. Chem. 689 (2004) 4729.
[8] E. Rosenberg, R. Kumar, Dalton Trans. 41 (2012) 714.
[9] R.J. Heetebrij, E.G. Talman, A.v. Velzen, R.P.M.v. Gijlswijk, S.S. Snoeijers, M. Schalk, J. Wiegant, F.v.d. Rijke, R.A.K. Kerkhoven, H.J. Tanke, J. Reedijk, H.J. Houthoff, ChemBioChem 4 (2003) 573.
[10] J.R.L. Priqueler, I.S. Butler, F.D. Rochon, Appl. Spectrosc. Rev. 41 (2006) 185–226.
[11] Materials Science and technology Group Oak Ridge National Laboratory P.O. Box 2008, Building 4515 1 Bethel Valley Road Oak Ridge, TN 37831–6071.
[12] B.F.G. Johnson, J. Lewis, J. Inorg. Synth. 13 (1972) 93.
[13] D.A. Horvat, E. Nordlander, M.G. Richmond, Organometallics 31 (2012) 6608.
[14] Antony J. Deeming, Kenneth I. Hardcastle, Shariff E. Kabir, J. Chem. Soc. Dalton Trans. Inorg. Chem. (1988) 827.
[15] X. Zhang, S. Kandala, L. Yang, W.H. Watson, X. Wang, D.A. Hrovat, W.T. Borden, M.G. Richmond, Organometallics 30 (2011) 1253.
[16] R. Persson, M. Monari, R. Gobetto, A. Russo Andrea, S. Aime, M.J. Calhorda, E. Nordlander, Organometallics 20 (20) (2001) 4150–4160.
[17] R. Persson, M.J. Stchedroff, B. Uebersezig, R. Gobetto, J.W. Steed, P.D. Prince, M. Monari, E. Nordlander, Organometallics 29 (2010) 2223.
[18] E. Rosenberg, S.E. Kabir, L. Milone, R. Gobetto, D. Osella, K.I. Hardcastle, S. Hajela, E. Wolf, K. Moizeau, D. Espisita, Organometallics 16 (1997) 2665.
[19] S. Kemmish, E. Rosenberg, unpublished results.
[20] E. Rosenberg, R. Kumar, W. Andregg, unpublished results.
[21] Oxford Nanopore Technologies.www.nanoporetech.com.